

# Dynamic Stability of Long, Axisymmetric Liquid Bridges

*This paper deals with the non-linear forced oscillations of axisymmetric long liquid bridges between equal disks. The dynamics of the liquid bridge has been analyzed by using a self-similar, one-dimensional model already used in similar problems. The influence of the dynamics on the static stability limits, as well as the main characteristics of the non-linear behaviour of long liquid bridges, have been studied within the range of validity of the mathematical model used here.*

## 1 Introduction

In the last years isothermal liquid bridges have focused the attention of many investigators, with a large number of published papers on this topic (a review of the literature related to liquid bridges can be found in *Sanz-Andres* [1]). Because of the large number of parameters involved, the study of liquid bridges becomes a formidable task which extends in time from the early paper of *Gillette and Dyson* [2] to the late paper of *Slobochanin and Perales* [3]. Most of these papers are only concerned with static stability limits. As far as we know only a few attempts have been made to analyze the influence of the dynamics of the liquid bridge, and these efforts have been centred more in the dynamics itself than in its influence on the stability limits (*Meseguer* [4], *Rivas and Meseguer* [5], *Perales and Meseguer* [6], *Sanz and López-Diez* [7], *Zhang and Alexander* [8], *Langbein* [9], *Schulkes* [10], among others).

In this paper the influence of the dynamics on the stability limits of liquid bridges is analyzed by using a simplified one-dimensional, self-similar model which, in spite of its simplicity, allows us to get some feeling on the dynamical behaviour of long liquid bridges. Associated with stability limits is the concept of stability margin, which has been defined as the difference between the energy of the stable equilibrium shape and of the unstable one for a given liquid bridge. The stability margin gives an estimate of the minimum energy which is needed to break a liquid bridge

through a given perturbation. Stability margins are discussed in sect. 2, whereas in sect. 3 the forced oscillations of long liquid bridges are analyzed, and stability diagrams for such kinds of perturbation are obtained.

## 2 Problem Formulation

The fluid configuration under consideration consists of an axisymmetric liquid bridge, with constant density  $\rho$ , kinematic viscosity  $\nu$  and surface tension  $\sigma$ , held by capillary forces between two coaxial, solid disks of radius  $R$  which are a distance  $L$  apart, as sketched in fig. 1. The volume of liquid,  $V'$ , is assumed to be almost the volume of a cylinder of the same  $R$  and  $L$ ,  $V' \approx \pi R^2 L$ , and it is also assumed that there is a small gravity field acting parallel to the liquid bridge axis. To describe the behaviour of such a fluid configuration the following dimensionless parameters are introduced: slenderness  $A = L/(2R)$ , dimensionless volume  $V = V'/R^3$ , Bond number  $B = \rho g R^2/\sigma$ , and viscosity parameter  $C = \nu(\rho/(\sigma R))^{1/2}$ . In addition to these parameters, it must be stated that all physical magnitudes used in the following have been made dimensionless by using  $R$  and  $(\rho R^3/\sigma)^{1/2}$  as characteristic length and characteristic time, respectively.

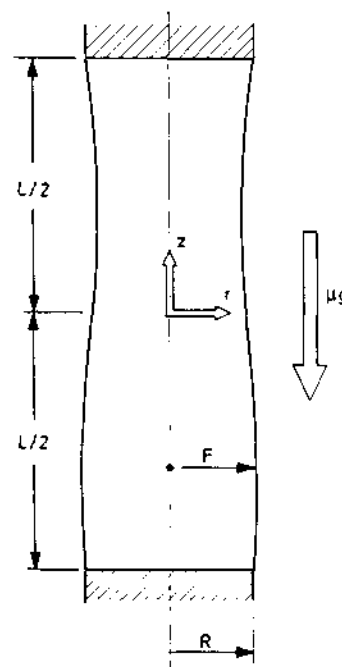


Fig. 1. Geometry and coordinate system for the liquid bridge problem

Mail address: Prof. J. Meseguer, M. A. González, Lamf, E.T.S.I. Aeronáuticos, Universidad Politécnica de Madrid, E-28040 Madrid, Spain; Dr. J. I. D. Alexander, Center for Microgravity and Materials Research (CMMR), The University of Alabama in Huntsville, Huntsville, AL 35899, USA.  
Paper submitted: May 25, 1993.  
Submission of final revised version: December 2, 1993.  
Paper accepted: January 7, 1994.

It has been demonstrated in *Rivas and Meseguer* [5] that close to the static stability limit of cylindrical liquid bridges ( $A \approx \pi$ ,  $B \approx 0$ ,  $V \approx 2\pi A$ ) there is a self-similar solution for the dynamics of the liquid bridge. These authors performed their analysis by using a one-dimensional model in which the axial velocity is assumed to be dependent on the axial coordinate  $z$  and the time  $t$ , but not on the radial coordinate  $r$  (such hypothesis has proved to be valid provided the slenderness is high enough, say  $A > 1.5$ , *Perales and Meseguer* [6]). Within the validity range of such analysis the variation with time of the interface deformation is given by the Duffing equation

$$\alpha_{tt} + \gamma \alpha_t - m\alpha - \alpha^3 = \bar{\beta} \tag{1}$$

where

$$\alpha = \frac{1}{4} A \left( \frac{1}{3} \delta \right)^{-1/2}, \quad \theta = \frac{2}{5} t (2\delta)^{1/2},$$

$$\gamma = \frac{5}{2} C (2\delta)^{-1/2}, \quad \bar{\beta} = \frac{1}{2} B \left( \frac{1}{3} \delta^3 \right)^{-1/2}, \tag{2}$$

are the self-similar variables and parameters. In these last expressions  $A$  is the amplitude of the interface deformation, which in this model varies as  $S(z, t) = 1 + A(t) \sin(\pi z)/A$  (formally  $A$  measures the deformation of a magnitude proportional to the liquid bridge cross-section,  $S = F^2$ ), whereas  $\delta$  stands for a reduced slenderness which includes volume effects:

$$-m\delta = 1 - \frac{A}{\pi} + \frac{1}{2} \left( \frac{V}{2\pi A} - 1 \right),$$

where  $\delta$  is positive and  $m$  takes account for the sign ( $m = \pm 1$ );  $t$  is the dimensionless time and the parameters  $C$  and  $B$  have been already defined.

To simplify the explanation, let us denote the self-similar variables and parameters involved in the problem, as defined by expressions (2), with labels indicating their main physical meaning, so that in the following we refer to  $\alpha$ ,  $\theta$ ,  $\gamma$ , and  $\bar{\beta}$  as deformation of the liquid bridge interface, time, viscosity, and Bond number, respectively. Let us also assume that gravity oscillates around some mean value, in such a way that in self-similar variables the time variation of the Bond number can be written as  $\bar{\beta} = \beta + b \cos(\Omega\theta)$ , where  $\Omega$  stands for the self-similar frequency of the imposed perturbation. In such a case eq. (1) would be

$$\alpha_{tt} + \gamma \alpha_t - m\alpha - \alpha^3 = \beta + b \cos(\Omega\theta), \tag{3}$$

which allows one to analyze, within the validity range of this model, both the static stability margin and the forced non-linear response of the liquid bridge.

Static stability margin results from eq. (3) taking  $b = 0$ . The potential energy of the liquid bridge, which accounts for both gravity field and surface energies, in self-similar variables will be

$$\xi = -\frac{1}{2} m\alpha^2 - \frac{1}{4} \alpha^4 - \beta\alpha, \tag{4}$$

where  $\xi$  is related to dimensionless energy (made dimensionless with  $\sigma R^2$ ) through the expression

$$\xi = \frac{16}{3} (\pi\delta)^{-2} (E - E_0) \tag{5}$$

$E_0$  accounting for all terms contributing to energy which do not depend on the interface deformation. Equilibrium shapes are given by

$$\frac{d^2\xi}{d\alpha^2} = -m\alpha - \alpha^3 - \beta = 0. \tag{6}$$

Eq. (6) has one real root if  $m = +1$ , which is unstable ( $d^2\xi/d\alpha^2 < 0$ ), and three real roots,  $\alpha_1 > \alpha_2 > \alpha_3$ , in the case  $m = -1$ . From these, the two extreme roots,  $\alpha_1$  and  $\alpha_3$ , correspond to unstable equilibrium shapes, whereas the central one represents a stable configuration. Thus, within this approximation the stability margin will be the difference between the energy of the unstable equilibrium shapes and of the stable one,  $\Delta\xi = \xi_{unstable} - \xi_{stable}$ . This behaviour is summarized in fig. 2, where the variation of the roots  $\alpha_1$ ,  $\alpha_2$ , and  $\alpha_3$  with  $\beta$  as well as the stability margins  $\Delta\xi_3 = \xi(\alpha_3) - \xi(\alpha_2)$  and  $\Delta\xi_1 = \xi(\alpha_1) - \xi(\alpha_2)$ , are shown. Obviously, the stability margin is defined by the smaller of such values,  $\Delta\xi_1$  in our case, which in the following will be denoted as  $\Delta\xi$ . According to eq. (5), in dimensionless variables the stability margin is given by  $\Delta E = \frac{3}{16} \pi^2 \Delta\xi \delta^2$ , that is, the stability margin is proportional to the square of the distance to the stability limit (such stability limit being  $\delta = 0$ ), the proportionality constant,  $\Delta\xi$ , being smaller as the Bond number increases. This factor, hence the stability margin, becomes zero when  $\beta = 2\sqrt{3}/9$ , which represents, when dimensionless variables are used, the variation with

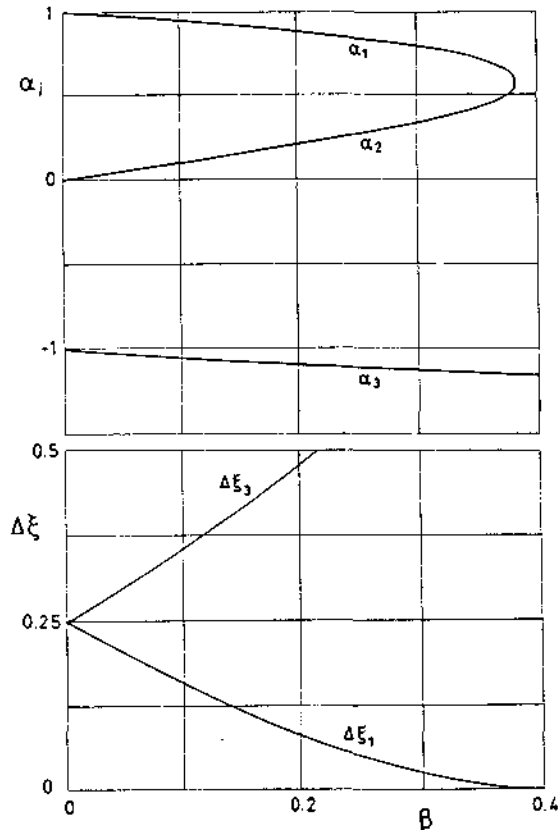


Fig. 2. Variation with the Bond number,  $\beta$ , of the roots,  $\alpha_i$ , of eq. (6), which define the equilibrium shapes of a slender liquid bridge, and variation with  $\beta$  of the difference,  $\Delta\xi_i$ , between the energy of each one of the unstable equilibrium shapes and of the stable one

Bond number of the stability limit of almost cylindrical liquid bridges,  $B = \frac{4}{3}\delta^{3/2}$ , already calculated by Vega and Perales [11].

### 3 Dynamic Stability

The stability margin or safety margin represents a limit to the minimum energy needed to break the liquid bridge. That means that, for a given perturbation, the response of the liquid bridge will depend on the energy of the perturbation; the liquid bridge will remain stable if the energy is smaller than the corresponding stability margin and it could be unstable if such energy becomes bigger. Of course in this last case the evolution of the liquid bridge depends on how the perturbation is imposed and on how such energy is dissipated because of viscosity. To fix our ideas let us consider the forced oscillation of the liquid bridge in gravitationless conditions ( $\beta = 0, b \neq 0$ ). In that case  $\alpha_2 = 0$  and  $\alpha_1 = -\alpha_3 = 1$ , so the  $\Delta\xi = \frac{1}{4}$ . The time variation of the interface is now defined by the expression

$$\alpha_{\theta\theta} + \gamma\alpha_{\theta} + \alpha - \alpha^3 = b \cos(\Omega\theta + \varphi), \tag{7}$$

which, assuming steady oscillations are reached, can be integrated in a first approximation [12] obtaining  $\alpha = a \cos(\Omega\theta)$ , where  $a$  is related to viscosity,  $\gamma$ , to the amplitude of the perturbation,  $b$ , and to the frequency of the perturbation,  $\Omega$ , through the equation

$$a^2 \left(1 - \Omega^2 - \frac{3}{4}a^2\right)^2 + \gamma^2 \Omega^2 a^2 = b^2. \tag{8}$$

Within this rough approximation (to write down eq. (8) a term in  $a^3 \cos(3\Omega\theta)$  has been neglected) the oscillation of the liquid bridge can be easily visualized by plotting the liquid bridge evolution in the phase space (deformation-velocity-energy diagram), as shown in fig. 3. Note that,

since we are considering an evolution, kinetic energy must be also taken into account, so that at every point of the phase space the energy will be the sum of the potential energy plus the kinetic energy:

$$\xi = \frac{1}{2}\alpha^2 - \frac{1}{4}\alpha^4 + \frac{1}{2}\alpha_{\theta}^2. \tag{9}$$

Two different oscillations of the liquid bridge, with amplitude  $a < 1$ , have been also represented in fig. 3, one corresponding to  $\Omega < 1$  and the other corresponding to  $\Omega > 1$ . Note that, for the movement under consideration, the energy of the liquid bridge, hence the energy of the perturbation, can be greater than that corresponding to the stability margin ( $\Delta\xi = \frac{1}{4}$ ) and the configuration remain stable, as it happens in the  $\Omega > 1$  case.

According to the plot of fig. 3, the liquid bridge will be unstable when  $a = 1$ , and, in that case, eq. (8) gives us the relationship between the viscosity  $\gamma$  and the parameters defining the perturbation

$$\gamma^2 = \Omega^{-2} \left[ b^2 - \left( \frac{1}{4} - \Omega^2 \right)^2 \right]. \tag{10}$$

Once  $b$  and  $\Omega$  are fixed, the liquid bridge evolution will be stable if the viscosity of the liquid is greater than the value resulting from eq. (10), otherwise it will be unstable. This behaviour is summarized in fig. 4, which has been plotted by using eq. (10). For a given viscosity  $\gamma$  and frequency  $\Omega$  the evolution will be unstable if the point representing this evolution lies on the left of the corresponding  $b$ -curve, and stable if the point lies on the right.

Of course, this description of the phenomenon must be regarded as qualitative only. The results obtained are based on the assumption that the response of the liquid bridge is co-sinusoidal ( $\alpha = a \cos(\Omega\theta)$ ) which, as already stated, is only a rough approximation to the solution of eq. (7).

To get more precise results, eq. (7) has been numerically integrated by using a fourth-order Runge-Kutta method and the trajectories in the phase-plane obtained. Depending on the values of the parameters involved ( $\gamma, b$ , and  $\Omega$ ) and the initial conditions these trajectories can be closed curves (the deformation of the liquid bridge interface,  $\alpha$ , remains bounded no matter what the value of  $\theta$  is) or the deformation continuously grows with time. The first case means that the liquid bridge is stable for the imposed perturbation, whereas in the second case the fluid configuration becomes unstable. The border between the two cases being the dynamic stability limit for the perturbation under consideration. When forced oscillations are considered the stability limit depends, as already stated, on the nature of the perturbation imposed and on the initial conditions. To avoid the influence of the starting transient, calculations have been performed as follows: first of all a set of values of the parameters  $\gamma, b$ , and  $\Omega$  for which the liquid bridge evolution is clearly stable is chosen (this is achieved by selecting a high value of viscosity  $\gamma$ ). Once a steady oscillation for the selected set of values of the parameters is reached, the value of one of the parameters is slightly changed (in our case the value of  $\gamma$  is slightly reduced at the beginning of a cycle); in this way initial conditions for the second set of values of the parameters are extremely close

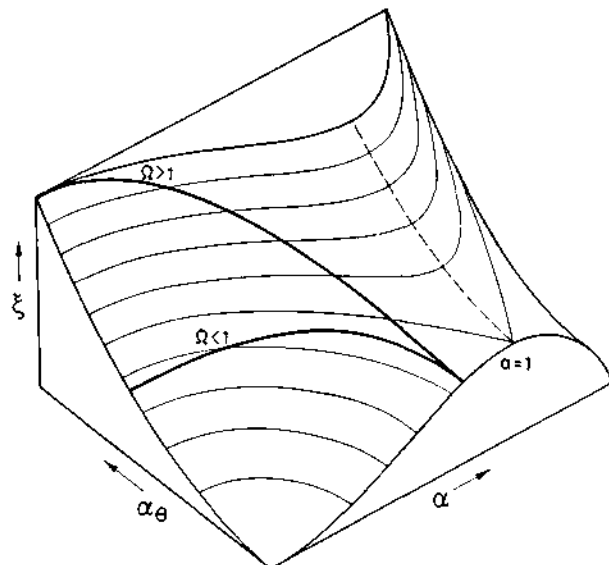


Fig. 3. Phase space (deformation of the interface,  $\alpha$ , velocity,  $\alpha_{\theta}$ , and energy,  $\xi$ ) of the forced oscillations of a liquid bridge according to the simplified model given by eq. (8). There are two evolutions represented in this plot,  $\Omega > 1$  and  $\Omega < 1$ , where  $\Omega$  stands for the pulsation of the forcing action

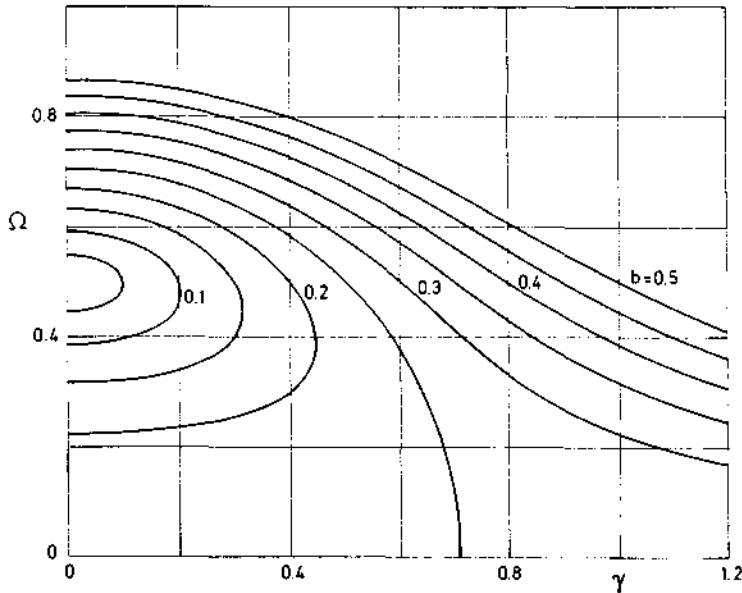


Fig. 4. Stability diagram in self-similar variables as given by eq. (10). Points at the left of each curve  $b = \text{const.}$  are unstable for this value of  $b$ , whereas those lying at the right are stable

to that corresponding to a steady oscillation and transient effects due to initial conditions can be made negligible.

The results obtained are shown in fig. 5. Also in this plot each one of the curves  $b = \text{const.}$  represents the corresponding stability limit. Points at the right of a given curve represent stable evolutions (high values of the viscosity,  $\gamma$ ) whereas those at the left side region (low values of  $\gamma$ ) correspond to unstable evolutions. Note that once  $\gamma$  and  $b$  are fixed there is one or even two sets of values of  $\Omega$  for which the liquid bridge evolution becomes unstable.

The response of the liquid bridge, defined as  $\alpha_m/b$  where  $\alpha_m$  stands for the maximum value of  $\alpha$  in each cycle, is shown in fig. 6 for different values of  $b$ .

To get an idea of the importance of initial conditions on the response of the liquid bridge eq. (7) has been integrated

again with initial conditions  $\alpha = 0, \alpha_0 = 0$ . The stability limit corresponding to  $b = 0.5$  obtained by using this initial-condition (curve labelled 2 in fig. 7) is compared with the calculated taking "steady" initial conditions (curve 1). Note that the influence of initial conditions becomes negligible when  $\Omega$  is small enough, but that differences can be remarkable as the value of  $\Omega$  increases.

Finally, it must be said that the Duffing equation, here used to analyze the non-linear forced oscillation of long liquid bridges, is a typical example of a non-linear oscillator in which chaos phenomena appear [13]. Such chaotic behaviour has been detected in our calculation, it clearly appears when both  $\Omega$  and  $\gamma$  are small, although no attempts have been made to perform a deep analysis of such behaviour, which is out of the scope of this paper.

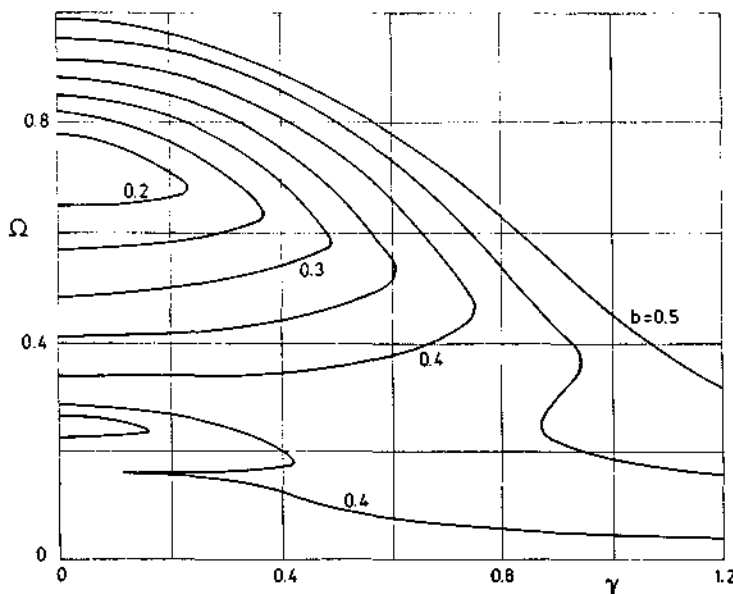


Fig. 5. Stability diagram in self-similar variables obtained by numerical integration of eq. (3). Points at the left of each curve  $b = \text{const.}$  are unstable for this value of  $b$ , whereas those lying at the right are stable

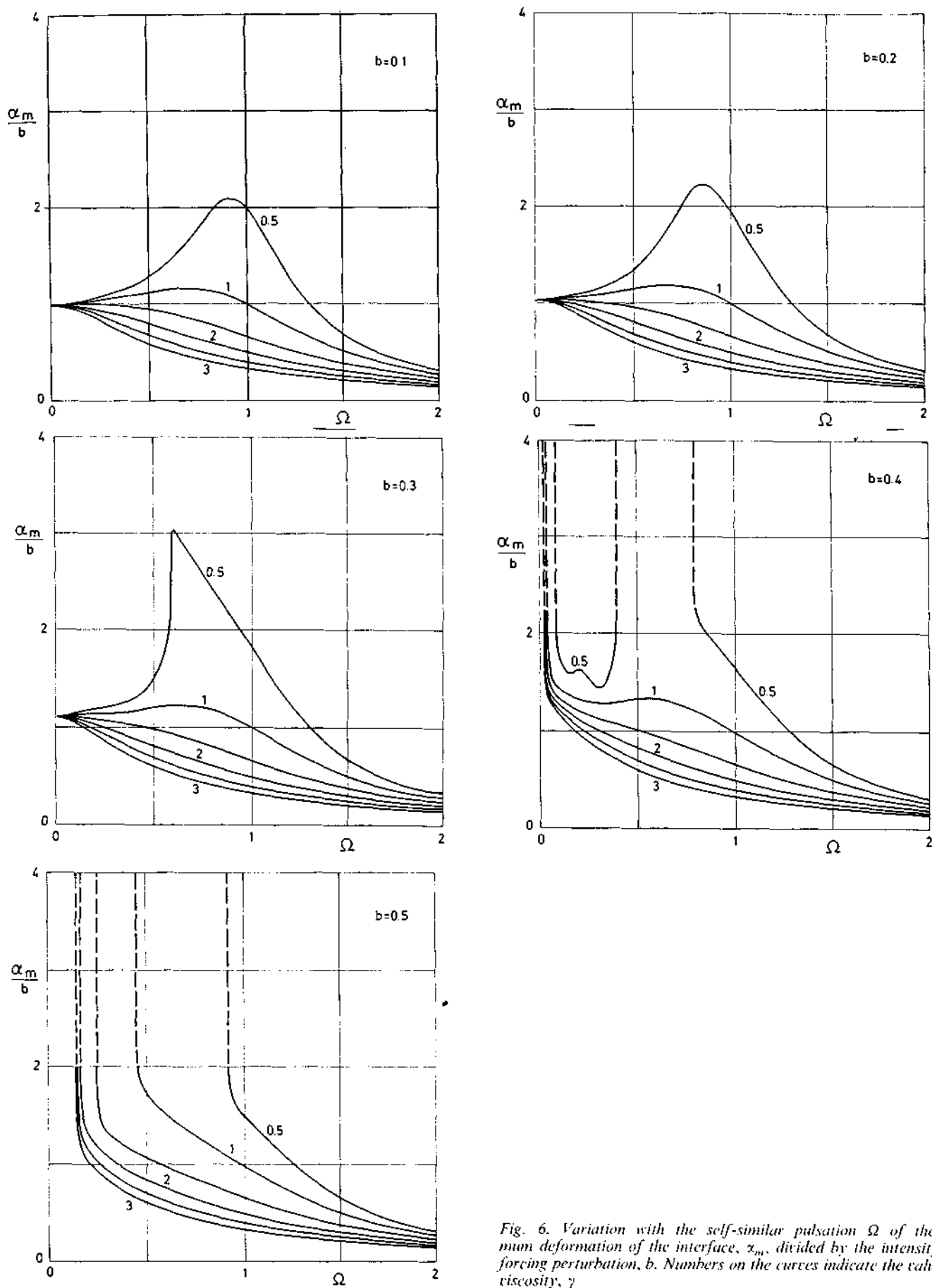


Fig. 6. Variation with the self-similar pulsation  $\Omega$  of the maximum deformation of the interface,  $\alpha_m$ , divided by the intensity of the forcing perturbation,  $b$ . Numbers on the curves indicate the value of the viscosity,  $\gamma$

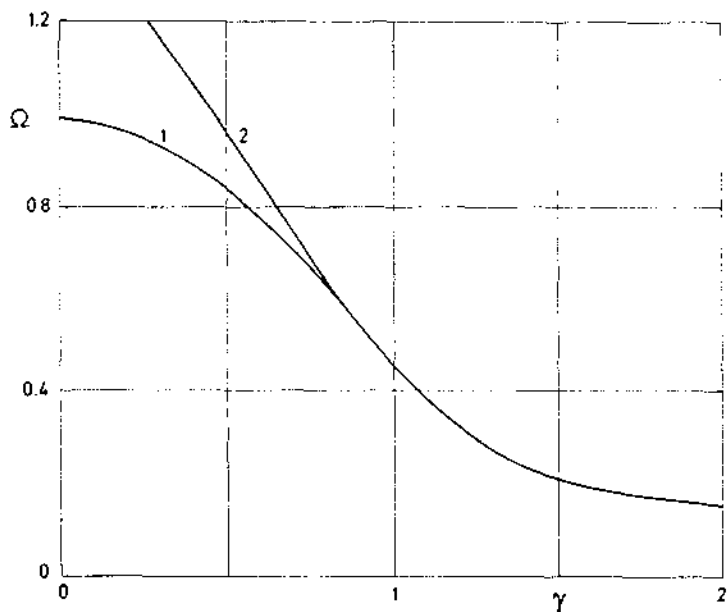


Fig. 7. Influence of the initial conditions on the stability diagram. Curves 1 and 2 have been obtained under different initial conditions as explained in the text

### Acknowledgments

This work has been supported by the Spanish Comisión Interministerial de Ciencia y Tecnología (CICYT) and is part of a more general endeavour for the study of fluid physics and materials processing under microgravity (Project No. ESP92-0001-CP).

### References

- 1 Sanz-Andres, A.: Static and Dynamic Response of Liquid Bridges; in *Microgravity Fluid Mechanics*, H. J. Rath (ed.), Springer-Verlag, Berlin, p. 3 (1992)
- 2 Gillette, R. D., Dyson, R. C.: Stability of Fluid Interfaces of Revolution Between Equal Solid Circular Plates. *Chem. Eng. J.*, vol. 2, p. 44 (1971)
- 3 Slobozhanin, L. A., Perales, J. M.: Stability of Liquid Bridges Between Equal Disks in an Axial Gravity Field. *Phys. Fluids A*, vol. 5, p. 1305 (1993)
- 4 Meseguer, J.: The Breaking of Axisymmetric Slender Liquid Bridges. *J. Fluid Mech.*, vol. 130, p. 123 (1983)
- 5 Rivas, D., Meseguer, J.: One-dimensional, Self-similar Solution of the Dynamics of Axisymmetric Slender Liquid Bridges. *J. Fluid Mech.*, vol. 138, p. 417 (1984)
- 6 Perales, J. M., Meseguer, J.: Theoretical and Experimental Study of the Vibration of Axisymmetric Viscous Liquid Bridges. *Phys. Fluids A*, vol. 4, p. 1110 (1992)
- 7 Sanz, A., López-Diez, J.: Non-axisymmetric Oscillations of Liquid Bridges. *J. Fluid Mech.*, vol. 205, p. 503 (1989)
- 8 Zhang, Y., Alexander, J. I. D.: Sensitivity of Liquid Bridges Subject to Axial Residual Acceleration. *Phys. Fluids A*, vol. 2, p. 1966 (1990)
- 9 Langbein, D.: Oscillations of Finite Liquid Columns. *Microgravity Sci. Technol.*, vol. 5, p. 73 (1992)
- 10 Schulkes, R. M. S. M.: Non Linear Liquid Bridge Dynamics. *ESA SP-333*, vol. 1, p. 61, ESA Publ. Div., ESTEC, Noordwijk (1992)
- 11 Vega, J. M., Perales, J. M.: Almost Cylindrical Isorotating Liquid Bridges for Small Bond Numbers. *ESA SP-191*, p. 247, ESA Publ. Div., ESTEC, Noordwijk (1992)
- 12 Stoker, J. J.: *Nonlinear Vibrations*, Vol. II, Interscience (1966)
- 13 Thompson, J. M. T., Steward, M. B.: *Nonlinear Dynamics and Chaos*, John Wiley & Sons Ltd., Chichester (1988)